REFERENCES AND NOTES

1. W. Kauzmann, *Adv. Protein Chem.* **14**, 1 (1959).
2. M. F. Perutz, J. C. Kendrew, H. C. Watson, *J. Mol. Biol.* **13**, 669 (1965).
3. B. Lee and F. M. Richards, *ibid.* **55**, 379 (1971).
4. C. Chothia, *ibid.* **105**, 1 (1976).
5. G. D. Rose *et al.*, *Science* **229**, 834 (1985).
6. S. Miller *et al.*, *J. Mol. Biol.* **196**, 641 (1987); J. Janin, S. Miller, C. Chothia, *ibid.* **204**, 155 (1988).
7. J. Kyte and R. F. Doolittle, *ibid.* **157**, 105 (1982).
8. D. Eisenberg, *Annu. Rev. Biochem.* **53**, 595 (1984); D. M. Engleman, T. A. Steitz, A. Goldman, *Annu. Rev. Biophys. Biophys. Chem.* **15**, 321 (1986).
9. D. M. Engelman and G. Zaccai, *Proc. Natl. Acad. Sci. U.S.A.* **77**, 5894 (1980).
10. J. Deisenhofer *et al.*, *J. Mol. Biol.* **180**, 385 (1984); *Nature* **318**, 618 (1985).
11. J. P. Allen *et al.*, *Proc. Natl. Acad. Sci. U.S.A.* **83**, 8589 (1986); J. P. Allen, G. Feher, T. O. Yeates, H. Komiya, D. C. Rees, *ibid.* **84**, 5730 (1987).
12. C.-H. Chang *et al.*, *FEBS Lett.* **205**, 82 (1986).
13. T. O. Yeates *et al.*, *Proc. Natl. Acad. Sci. U.S.A.* **84**, 6438 (1987).
14. D. Eisenberg and A. D. McLachlan, *Nature* **319**, 199 (1986).
15. D. Eisenberg, R. M. Weiss, T. C. Terwilliger, W. Wilcox, *Faraday Symp. Chem. Soc.* **17**, 109 (1982); Hydrophobicities are: Ala, 0.25; Arg, −1.76; Asn, −0.64; Asp, −0.72; Cys, 0.04; Glu, −0.62; Gln, −0.69; Gly, 0.16; His, −0.40; Ile, 0.73; Leu, 0.53; Lys, −1.10; Met, 0.26; Phe, 0.61; Pro, −0.07; Ser, −0.26; Thr, −0.18; Trp, 0.37; Tyr, 0.02; and Val, 0.54.
16. H. Komiya *et al.*, *Proc. Natl. Acad. Sci. U.S.A.* **85**, 9012 (1988).
17. H. G. Khorana, *J. Biol. Chem.* **263**, 7439 (1988); A. Blanck and D. Oesterhelt, *EMBO J.* **6**, 265 (1987).
18. J. Nathans and D. S. Hogness, *Cell* **34**, 807 (1983); A. F. Cowman, C. S. Zuker, G. M. Rubin, *ibid.* **44**, 705 (1986); D. Young, G. Waitches, C. Birchmeier, O. Fasano, M. Wigler, *ibid.* **45**, 711 (1986); J. Nathans, D. Thomas, D. S. Hogness, *Science* **232**, 193 (1986); B. K. Kobilka *et al.*, *ibid.* **238**, 650 (1987); T. I. Bonner, N. J. Buckley, A. C. Young, M. R. Brann, *ibid.* **237**, 527 (1987); D. Julius, A. B. MacDermott, R. Axel, T. M. Jessel, *ibid.* **241**, 558 (1988); J. Nathans and D. S. Hogness, *Proc. Natl. Acad. Sci. U.S.A.* **81**, 4851 (1984); Y. Yarden *et al.*, *ibid.* **83**, 6795 (1986); T. Frielle *et al.*, *ibid.* **84**, 7920 (1987); J. Gocayne *et al.*, *ibid.*, p. 8296; K. J. Fryxell and E. M. Meyerowitz, *EMBO J.* **6**, 443 (1987); E. G. Peralta *et al.*, *ibid*, p. 3923; R. A. F. Dixon *et al.*, *Nature* **321**, 75 (1986); T. Kubo *et al.*, *ibid.* **323**, 411 (1986); Y. Masu *et al.*, *ibid.* **329**, 836 (1987); P. R. Schofield, L. M. Rhee, E. G. Peralta, *Nucleic Acids Res.* **15**, 3636 (1987); T. Kubo *et al.*, *FEBS Lett.* **209**, 367 (1986).
19. T. Kayano, M. Noda, V. Flockerzi, H. Takahashi, S. Numa, *FEBS Lett.* **228**, 187 (1988); T. Tanabe *et al.*, *Nature* **328**, 313 (1987).
20. G. Hauska, W. Nitschke, R. G. Herrmann, *J. Bioenerg. Biomembr.* **20**, 211 (1988).
21. J. Bollinger *et al.*, *Proc. Natl. Acad. Sci. U.S.A.* **81**, 3287 (1984); A. Krikos, N. Mutoh, A. Boyd, M. I. Simon, *Cell* **33**, 615 (1983).
22. J. Devereux, P. Haeberli, O. Smithies, *Nucleic Acid Res.* **12**, 387 (1984); M. Gribskov, A. D. McLachlan, D. Eisenberg, *Proc. Natl. Acad. Sci. U.S.A.* **84**, 4355 (1987).
23. E. L. Smith, *Harvey Lect.* **62**, 231 (1967); C. Chothia and A. M. Lesk, *EMBO J.* **5**, 823 (1986); J. F. Reidhaar-Olson and R. T. Sauer, *Science* **241**, 53 (1988).
24. D. C. Rees, H. Komiya, T. O. Yeates, J. P. Allen, G. Feher, *Annu. Rev. Biochem.* **58**, 607 (1989).
25. D. Eisenberg, R. M. Weiss, T. C. Terwilliger, *Proc. Natl. Acad. Sci. U.S.A.* **81**, 140 (1984).
26. J. L. Cornette *et al.*, *J. Mol. Biol.* **195**, 659 (1987).
27. A. M. Lesk and C. Chothia, *ibid.* **136**, 225 (1980).
28. We thank J. P. Allen and G. Feher for helpful discussions. Supported by NIH grants GM31299 and GM39558. D.C.R. is an A. P. Sloan research fellow. Programs and sequence alignments used in this work are available from D.C.R.

3 March 1989, accepted 2 June 1989

Interpretation of Cloud-Climate Feedback as Produced by 14 Atmospheric General Circulation Models

R. D. CESS, G. L. POTTER, J. P. BLANCHET, G. J. BOER, S. J. GHAN, J. T. KIEHL, H. LE TREUT, Z.-X. LI, X.-Z. LIANG, J. F. B. MITCHELL, J.-J. MORCRETTE, D. A. RANDALL, M. R. RICHES, E. ROECKNER, U. SCHLESE, A. SLINGO, K. E. TAYLOR, W. M. WASHINGTON, R. T. WETHERALD, I. YAGAI

Understanding the cause of differences among general circulation model projections of carbon dioxide–induced climatic change is a necessary step toward improving the models. An intercomparison of 14 atmospheric general circulation models, for which sea surface temperature perturbations were used as a surrogate climate change, showed that there was a roughly threefold variation in global climate sensitivity. Most of this variation is attributable to differences in the models' depictions of cloud-climate feedback, a result that emphasizes the need for improvements in the treatment of clouds in these models if they are ultimately to be used as climatic predictors.

OBSERVED AND PROJECTED INcreases in the concentration of atmospheric CO_2 and other greenhouse gases have stimulated considerable interest in modeling climatic change. The most detailed climate models for this purpose are three-dimensional general circulation models (GCMs). Although most GCMs are of similar design, there are significant differences among GCM projections of climatic warming as induced by increasing levels of atmospheric carbon dioxide (*1, 2*). The reasons for these differences are not fully understood, but variations in how cloud-climate feedback processes are simulated in the various models are thought to be largely responsible (*3*); cloud feedback is dependent on all aspects of a model and not just on cloud formation parameterizations. Clearly there is a need to isolate and to understand better cloud feedback mechanisms in GCMs, and, more specifically, to determine if they are a significant cause of intermodel differences in recent climate-change projections. Consequently we have made an intercomparison of cloud feedback in 14 atmospheric GCMs as part of a larger study directed toward improving GCMs and climatic projections.

Many facets of the climate system are not well understood, and thus the uncertainties in modeling atmospheric, cryospheric, and oceanic interactions are large. In evaluating the differences among models, we have focused first on atmospheric processes, because these uncertainties must be understood before others can be addressed. For simplicity, we have emphasized solely global-average quantities, and we adopted the conventional interpretation of climate change as a two-stage process: forcing and response (*4*). The concept of global-average forcing and response has proven useful in earlier interpretations of cloud-climate feedback. For example, by performing two GCM simulations for a doubling of atmospheric CO_2 concentration, one with computed clouds and the other with clouds that were invariant to the change in climate, Wetherald and Manabe have suggested (*5*) that cloud-climate feedback amplifies global warming by the factor 1.3. A somewhat larger amplification (1.8) was estimated by Hansen *et al.* (*6*) using a one-dimensional climate model to evaluate climate feedback mechanisms in a different GCM.

The global-mean direct radiative forcing, G, of the surface-atmosphere system is evaluated by holding all other climate parameters fixed. It is this quantity that induces the ensuing climate change, and physically it represents a change in the net (solar plus infrared) radiative flux at the top of the atmosphere (TOA). For an increase in the CO_2 concentration of the atmosphere, G is the reduction in the emitted TOA infrared flux resulting solely from the CO_2 increase, and this reduction results in a heating of the surface-atmosphere system. The response

R. D. Cess, Institute for Atmospheric Sciences, State University of New York, Stony Brook, NY 11794.
G. L. Potter, S. J. Ghan, K. E. Taylor, Lawrence Livermore National Laboratory, Livermore, CA 94550.
J. P. Blanchet and G. J. Boer, Canadian Climate Centre, Downsview, Ontario M3H 574, Canada.
J. T. Kiehl, A. Slingo, W. M. Washington, National Center for Atmospheric Research, Boulder, CO 80307.
H. Le Treut and Z.-X. Li, Laboratoire de Météorologie Dynamique, 24 Rue Lhomond, 75231 Paris Cédex 05, France.
X.-Z. Liang, Institute of Atmospheric Physics, Beijing, China.
J. F. B. Mitchell, United Kingdom Meteorological Office, Bracknell, Berkshire RG12 25, England.
J.-J. Morcrette, European Centre for Medium-Range Weather Forecasts, Reading, Berkshire RG2 9AX, England.
D. A. Randall, Colorado State University, Fort Collins, CO 80523.
M. R. Riches, Department of Energy, Washington, DC 20545.
E. Roeckner and U. Schlese, University of Hamburg, Bundesstrasse 55, D2000, Hamburg 13, Federal Republic of Germany.
R. T. Wetherald, Geophysical Fluid Dynamics Laboratory, Princeton University, Princeton, NJ 08540.
I. Yagai, Meteorological Research Institute of Japan, Ibaraki-Ken, 305 Japan.

process is the change in climate that is then necessary to restore the TOA radiation balance, such that

$$G = \Delta F - \Delta Q \quad (1)$$

where F and Q respectively denote the global-mean emitted infrared and net downward solar fluxes at the TOA. Thus ΔF and ΔQ represent the climate-change TOA responses to the direct radiative forcing G, and these are the quantities that are impacted by climate feedback mechanisms. Furthermore, it readily follows that the change in surface climate, expressed as the change in global-mean surface temperature ΔT_s, is related to the direct radiative forcing G by

$$\Delta T_s = \lambda G \quad (2)$$

where λ is the climate sensitivity parameter

$$\lambda = \frac{1}{\Delta F/\Delta T_s - \Delta Q/\Delta T_s} \quad (3)$$

An increase in λ thus represents an increased climate change due to a given climate forcing G.

A simple example illustrates the use of λ for evaluating feedback mechanisms. If only the basic temperature-radiation negative feedback exists, then climate change refers solely to temperature change, and there are no related changes in atmospheric composition, lapse rate (vertical temperature gradient), or surface albedo (reflectance). Thus $\Delta Q/\Delta T_s = 0$, and $\Delta F/\Delta T_s$ is evaluated with the assumption that $F = \varepsilon\sigma T_s^4$ (*7*), where σ is the Stefan-Boltzmann constant and ε is the emissivity of the surface-atmosphere system, which is constant in this case. It then follows that $\Delta F/\Delta T_s = 4F/T_s = 3.3$ W m^{-2} K^{-1} for conditions typical of Earth, so that in the absence of interactive feedback mechanisms, $\lambda = 0.3$ K m^2 W^{-1}.

A well-known positive feedback mechanism is water-vapor feedback (*8*), in which a warmer atmosphere contains more water vapor, which as a greenhouse gas amplifies the initial warming. Climate models that contain this positive feedback process typically give $\Delta F/\Delta T_s \simeq 2.2$ W m^{-2} K^{-1}. In addition, the increased water vapor increases the atmospheric absorption of solar radiation, and for a typical model this positive feedback yields $\Delta Q/\Delta T_s \simeq 0.2$ W m^{-2} K^{-1}. Thus, with the inclusion of water-vapor feedback λ is increased from 0.3 to 0.5 K m^2 W^{-1}.

Whereas water-vapor feedback is intuitively straightforward to understand, cloud feedback is a far more complex phenomenon. There are several ways that clouds can produce feedback mechanisms. For example, if global cloud amount decreases because of climate warming, as occurred in simulations with the 14 GCMs we employed, then this decrease reduces the infrared greenhouse effect attributed to clouds. Thus as Earth warms it is able to emit infrared radiation more efficiently, moderating the global warming and so acting as a negative climate feedback mechanism. But there is a related positive feedback: the solar radiation absorbed by the surface-atmosphere system increases because the diminished cloud amount causes a reduction of reflected solar radiation by the atmosphere. The situation is further complicated by climate-induced changes in both cloud vertical structure and cloud optical properties, which result in additional infrared and solar feedbacks (*2*).

In our intercomparison, cloud effects were isolated by separately averaging a model's clear-sky TOA fluxes (*2, 9*), such that in addition to evaluating climate sensitivity for the globe as a whole, we were also able to consider an equivalent "clear-sky" Earth. In other words, a model's clear-sky TOA infrared and solar fluxes were separately stored during integration and then globally averaged by use of conventional latitudinal area weighting. When used in conjunction with Eq. 3, a single model integration thus provided not only the global climate sensitivity parameter but also a second sensitivity parameter that refers to a clear-sky Earth with the same climate as that with clouds present. In effect, we processed GCM output in a manner similar to the way in which data is processed in the Earth Radiation Budget Experiment (*10*), an experiment that also produces an equivalent clear-sky Earth.

Our choice of a model intercomparison simulation was governed by several factors. Ideally the climate simulation should refer to a relevant situation, such as increasing the atmospheric CO_2 concentration. Only 3 of the 14 models, however, have been employed for this purpose. Furthermore, these three models have, at least in part, differing climate sensitivities because their control (that is, present-day) climates are different (*2, 3*). If a model produces a control climate that is either too warm or too cold, then it will respectively produce a climate sensitivity parameter that is too small or too large, and clearly the intercomparison simulation had to be designed to eliminate this effect. There was also a practical constraint: the CO_2 simulations require large amounts of computer time for equilibration of the rather primitive ocean models that have been used in these numerical experiments.

As an alternative that eliminated both of the above-mentioned difficulties, we adopted ± 2 K sea surface temperature (SST) perturbations, in conjunction with a perpetual July simulation, as a surrogate climate change for the sole purpose of intercomparing climate sensitivity (*2*). This procedure is in essence an inverse climate change simulation. Rather than introducing a forcing G into the models and then letting the climate respond to this forcing, we instead prescribed the climate change and let the models in turn produce their respective forcings in accordance with Eq. 1. This procedure eliminated the substantial computer time required for equilibration of the ocean. The second advantage was that because the same SSTs were prescribed (*11*), all of the models had essentially the same control climate because land temperatures are tightly coupled, through atmospheric transport, to the SSTs. The models then all produced a global-mean ΔT_s between the -2 K and $+2$ K SST perturbation simulations that was close to 4 K, and different model sensitivities in turn resulted in different values for G.

The perpetual July simulation eliminated another problem. Our study focused solely on atmospheric feedback mechanisms, and inspection of output from all the models

Table 1. Summary of the GCMs used in the intercomparison (*13*). There are two GFDL models. NCAR, National Center for Atmospheric Research.

Model	Investigators
Canadian Climate Center (CCC)	Boer and Blanchet
Colorado State University (CSU)	Randall
European Centre for Medium-Range Weather Forecasts (ECMWF)	Morcrette
European Centre for Medium-Range Weather Forecasts–University of Hamburg (ECMWF/UH)	Roeckner and Schese
Geophysical Fluid Dynamics Laboratory (GFDL I and II)	Wetherald
Laboratoire de Météorologie Dynamique (LMD)	Le Treut and Li
Meteorological Research Institute of Japan (MRI)	Yagai
NCAR Community Climate Model, version 0 (CCMO)	Washington
NCAR Community Climate Model, version 1 (CCM1)	Slingo and Kiehl
NCAR Community Climate Model–Lawrence Livermore National Laboratory (CCM/LLNL)	Ghan and Taylor
Oregon State University–Institute for Atmospheric Physics, Beijing (OSU/IAP)	Liang
Oregon State University–Lawrence Livermore National Laboratory (OSU/LLNL)	Cess and Potter
United Kingdom Meteorological Office (UKMO)	Mitchell

showed that climate feedback caused by changes in snow and ice coverage was suppressed through use of a fixed sea ice constraint and because the perpetual July simulations produced little snow cover in the Northern Hemisphere. For this reason we adopted global averages rather than the 60°S to 60°N averages used in an earlier study (*2*).

Several of the 14 GCMs used in the intercomparison (designated by acronyms in Table 1) have common origins. The GFDL II model, relative to GFDL I, includes a parameterization for cloud albedo as a function of cloud water content. The CCM0 and CCM1 are the standard versions (0 and 1) of the NCAR CCM, with version 1 containing a revised radiation code. The CCM/LLNL GCM is CCM1 with a further solar radiation code revision and the incorporation of cloud albedos as a function of cloud water content. The OSU/IAP and OSU/LLNL GCMs are two-level models that contain modifications to the standard Oregon State University GCM. Both the numerical technique and the convective adjustment parameterization were revised in the OSU/IAP model, whereas the solar radiation code was revised in the OSU/LLNL GCM. The ECMWF GCM, relative to ECMWF/UH, has a revised radiation code and a smaller (factor of 2) horizontal resolution.

All of the models treat two cloud types: stratiform (large-scale) and convective clouds. Except in the ECMWF and ECMWF/UH models, stratiform clouds are formed in a vertical atmospheric layer when the relative humidity exceeds a prescribed threshold value, which varies among models for 90 to 100%. The models then either prescribe the cloud cover in their respective grid areas, which vary in size from 2.8° by 2.8° to 5° by 7.5° in latitude by longitude, or calculate it as a function of relative humidity. In the ECMWF and ECMWF/UH GCMs, vertical velocity and lapse rate are also used as cloud predictors.

The procedure for convective clouds is far less consistent. The CCC, the two GFDL, and the three CCM GCMs generate convective clouds in the same way as they generate stratiform clouds. However, the fraction of the grid area that is covered by convective cloud varies from 30 to 100% among these models. In the remaining models a parameterization is used that relates the convective cloud fraction to the convective precipitation rate.

In the intercomparison of climate sensitivity parameters, there was a nearly threefold variation in the global sensitivity parameter (Table 2), but excellent agreement in the clear sensitivity parameter. These clear values are also consistent with our conventional interpretation of water-vapor feedback as discussed above. These results suggest that the substantial disagreements in global sensitivity can largely be attributed to differences in cloud feedback. Understanding this point requires definitions of cloud feedback and cloud-radiative forcing. Cloud feedback has been discussed for roughly two decades, but there is considerable uncertainty as to its meaning; it has often been confused with cloud-radiative forcing, whereas it is actually related to a change in cloud-radiative forcing.

Cloud-radiative forcing refers to the radiative impact of clouds on the earth's radiation budget as determined at the TOA. Denoting this impact as *CRF*, and letting the subscript *c* refer to clear-sky fluxes, then

$$CRF = F_c - F + Q - Q_c \qquad (4)$$

In this definition *CRF* is positive when clouds produce a warming of the surface-atmosphere system. Combination of Eqs. 1, 2, 3, and 4 then yields

$$\lambda/\lambda_c = 1 + \Delta CRF/G \qquad (5)$$

where ΔCRF is the change in cloud-radiative forcing as induced by the change in climate and λ_c is the clear-sky climate sensitivity parameter (Table 2).

Conceptually cloud feedback should be related to a change in cloud-radiative forcing, as illustrated in Eq. 5. In the absence of cloud feedback (that is, $\Delta CRF = 0$), the global sensitivity parameter equals that for clear skies. In turn, a departure of λ/λ_c from unity is a measure of cloud feedback, and a $\lambda/\lambda_c > 1$ denotes a positive feedback. Cloud-radiative forcing for Earth's present climate is a measurable quantity; the Earth Radiation Budget Experiment (ERBE) is currently producing this information (*10*).

Table 2. Summary of climate sensitivity parameters for the perpetual July simulations; λ_c is the clear-sky sensitivity parameter.

Model	λ (K m^2 W^{-1})	λ_c (K m^2 W^{-1})	λ/λ_c
CCC	0.39	0.42	0.93
ECMWF	0.40	0.57	0.70
GFDL II	0.45	0.46	0.98
CSU	0.50	0.46	1.09
OSU/LLNL	0.52	0.48	1.08
MRI	0.60	0.47	1.28
GFDL I	0.60	0.48	1.25
UKMO	0.61	0.53	1.15
CCM1	0.70	0.43	1.63
CCM/LLNL	0.76	0.49	1.55
LMD	0.90	0.42	2.14
OSU/IAP	0.90	0.44	2.05
ECMWF/UH	1.11	0.47	2.36
CCMO	1.11	0.45	2.47
Mean	0.68	0.47	
SD	0.24	0.04	

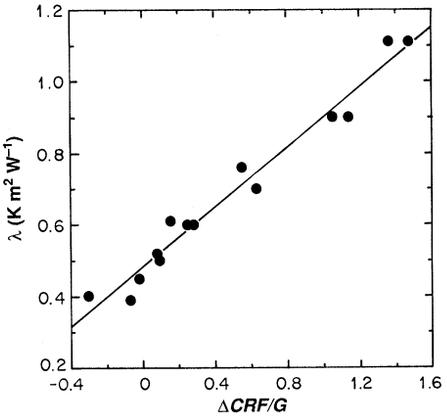

Fig. 1. The global sensitivity parameter λ plotted against the cloud feedback parameter $\Delta CRF/G$ for the 14 GCM simulations. The solid line represents a best-fit linear regression.

Equation 5 provides a convenient means of understanding why cloud feedback is the primary cause of the intermodel variations in global climate sensitivity. A scatter plot of λ versus the cloud feedback parameter $\Delta CRF/G$ for the 14 GCMs (Fig. 1) clearly shows that the intermodel differences in global climate sensitivity are dominated by their corresponding differences in $\Delta CRF/G$: the points scatter about a regression line that is consistent with Eq. 5. The scatter results from the relatively minor intermodel differences in the clear sensitivity parameter. This analysis thus supports the suggestion that cloud-climate feedback is a significant cause of intermodel differences in climate change projections.

The GFDL I and II models provide a direct means of appraising a specific cloud feedback component attributed to cloud optical properties. In GFDL II the cloud albedos are dependent on cloud water content, whereas in GFDL I these albedos are prescribed. Because cloud water content should, on average, increase as the climate warms, producing a related increase in cloud albedos, GFDL II should have, relative to GFDL I, a negative cloud feedback component (*12*). The global sensitivity parameter for GFDL II is 25% less than that for GFDL I (Table 2), consistent with this expectation.

A similarly straightforward argument does not, however, apply to the CCM1 versus CCM/LLNL models, for which the latter also incorporates cloud albedos that are dependent on cloud water content. An inspection of the output of these two GCMs shows, like the GFDL comparison, that CCM/LLNL contains, relative to CCM1, a negative solar cloud feedback component. But unlike the case for GFDL I and II, this negative feedback is compensated for by a positive cloud-amount feedback. The net

result is that the two models produced nearly identical cloud feedback, as shown by their similar λ/λ_c values (Table 2). Nor is it possible to segregate the 14 GCMs into low- and high-sensitivity groups on the basis of whether they do or do not incorporate cloud optical properties that depend upon cloud water content. The ECMWF and ECMWF/UH GCMs also incorporate this effect, and they lie at opposite ends of the cloud feedback spectrum (Table 2). Furthermore, even though the CSU and OSU/LLNL GCMs produced nearly identical modest positive cloud feedback (Table 2), this was actually a result of compensation between vastly different cloud feedback components.

In summary, although the 14 atmospheric GCMs produced comparable clear-sky sensitivity parameters, when cloud feedback was included, compatibility vanished and there was a nearly threefold variation in climate sensitivity as produced by the models. The cloud feedback ranged from modest negative to strong positive feedback. Clearly improvements in the treatment of clouds in GCMs are needed. But there are many other facets of a GCM, in addition to cloud optical properties and cloud formation parameterizations, that can influence cloud-climate interactions. The hydrological cycle, to cite one example, will most certainly play a dominant role.

Many of these GCMs are in a continual state of evolution. Thus this intercomparison is a snapshot that might no longer represent a specific model. Furthermore, these model-produced cloud feedbacks may not be representative of how the models would behave under realistic climate change conditions when they are coupled with interactive cryosphere and ocean models. Perpetual July simulations cannot be used for this purpose. Nor can the uniform SST perturbations, because they do not account for changes in equator-to-pole temperature gradients associated with actual climate change. For example, it has recently been speculated (*10*) that this latter effect, by itself, may produce a cloud feedback component resulting from latitudinal shifts in general circulation patterns. But these caveats do not alter our conclusion that 14 different GCMs produced a broad spectrum of cloud-climate feedback.

Climate research benefits from a diversity of climate models. If only a limited number of models were available, we could not confidently conclude that the role of cloud feedback is a key issue for climate studies. Before this study, only two GCMs had been used to provide estimates of cloud feedback (*5, 6*), and these two estimates showed much closer agreement than we have demonstrated.

REFERENCES AND NOTES

1. M. E. Schlesinger and J. F. B. Mitchell, *Rev. Geophys.* **25**, 760 (1987).
2. R. D. Cess and G. L. Potter, *J. Geophys. Res.* **93**, 8305 (1988).
3. Another important cause of these differences is that different climate models produce different control (that is, present-day) climates. For example, see (*2*); M. J. Spelman and S. Manabe, *J. Geophys. Res.*, **89**, 57 (1984).
4. R. E. Dickinson, in *Carbon Dioxide Review*, W. C. Clark, Ed. (Clarendon, New York, 1982), pp. 101–133; G. L. Potter and R. D. Cess, *J. Geophys. Res.* **89**, 9521 (1984).
5. R. T. Wetherald and S. Manabe, *J. Atoms. Sci.* **45**, 1397 (1988).
6. J. Hansen *et al.*, in *Climate Processes and Climate Sensitivity*, J. E. Hansen and T. Takahashi, Eds. (American Geophysical Union, Washington, DC, 1984), pp. 130–163. Hansen *et al.* indicated a feedback amplification due to clouds of 1.3 in their GCM study, but this value is for the absence of other feedback mechanisms. When water vapor and snow-ice feedbacks were included, their results implied a cloud feedback amplification of 1.8.
7. R. D. Cess, *J. Atmos. Sci.* **33**, 1831 (1976).
8. S. Manabe and R. T. Wetherald, *ibid.* **24**, 241 (1967).
9. T. P. Charlock and V. Ramanathan, *ibid.* **42**, 1408 (1985); V. Ramanathan, *J. Geophys. Res.* **92**, 4075 (1987).
10. V. Ramanathan *et al.*, *Science* **243**, 57 (1989).
11. R. C. Alexander and R. L. Mobley, *Mon. Weather Rev.* **104**, 143 (1976).
12. V. K. Petukhov *et al.*, *Izv. Acad. Sci. U.S.S.R. Atmos. Oceanic Phys.* **11**, 802 (1975); R. C. J. Somerville and L. A. Remer, *J. Geophys. Res.* **89**, 9668 (1984); M. E. Schlesinger, *Nature* **333**, 303 (1988).
13. A brief description of the 14 GCMs will be provided in Cess *et al.* (in preparation); descriptions of individual models are available from the respective investigators.

14. Valuable insights and suggestions were provided by W. L. Gates and M. E. Schlesinger. This study represents one of several Department of Energy model intercomparison projects, and it was performed under the auspices of the CO_2 Research Division, Office of Basic Energy Sciences, U.S. Department of Energy contract W-7405-ENG-48 to Lawrence Livermore National Laboratory, grant DEFG0285ER60314 to SUNY Stony Brook, and contract DE-AI01-80EV10220 to the National Center for Atmospheric Research, which is sponsored by the National Science Foundation. Further support was provided by the National Aeronautics and Space Administration Climate Program grant NAG 5-1058 to Colorado State University, and by the Bundeminister für Forschung and Technologie, Federal Republic of Germany, grant KF20128 to the University of Hamburg.

10 March 1989; accepted 20 June 1989

β-Adrenergic Inhibition of Cardiac Sodium Channels by Dual G-Protein Pathways

BERND SCHUBERT, ANTONIUS M. J. VANDONGEN, GLENN E. KIRSCH, ARTHUR M. BROWN

The signaling pathways by which β-adrenergic agonists modulate voltage-dependent cardiac sodium currents are unknown, although it is likely that adenosine 3′5′-monophosphate (cAMP) is involved. Single-channel and whole-cell sodium currents were measured in cardiac myocytes and the signal transducing G protein G_s was found to couple β-adrenergic receptors to sodium channels by both cytoplasmic (indirect) and membrane-delimited (direct) pathways. Hence, G_s can act on at least three effectors in the heart: sodium channels, calcium channels, and adenylyl cyclase. The effect on sodium currents was inhibitory and was enhanced by membrane depolarization. During myocardial ischemia the sodium currents of depolarized cells may be further inhibited by the accompanying increase in catecholamine levels.

IN THE LEXICON OF NEUROMODULATION, voltage-dependent Na^+ channels receive far less attention than voltage-dependent K^+ or Ca^{2+} channels, possibly because of the all-or-none nature of the propagated action potential. Previous studies, however, have shown that (i) the β-adrenergic agonist isoproterenol (ISO) decreases maximum upstroke velocity in depolarized ventricular myocytes (*1*); (ii) cAMP-dependent phosphorylation reduces neurotoxin-activated $^{22}Na^+$ flux (*2*) and promotes inactivation in embryonic rat brain cells (*2*); and (iii) cAMP modulates Na^+ currents in frog node of Ranvier (*2*). These studies suggest that a signal transducing G protein may link β-adrenergic receptors to Na^+ channels. To test this possibility, we examined the effects of ISO on Na^+ currents by whole-cell and single-channel recording in neonatal ventricular myocytes from rat.

ISO (1 μ*M*) applied extracellularly reduced whole-cell Na^+ current (I_{Na}) by 40.8 ± 17.5% (mean ± SD, $n = 4$) when I_{Na} was partially inactivated at a holding potential (HP) of −60 mV (Fig. 1A). The decrease began without measurable delay, was half maximal at about 5 s, peaked at about 15 s (Fig. 1A), and occurred without an

B. Schubert, Department of Molecular Physiology and Biophysics, Baylor College of Medicine, One Baylor Plaza, Houston, TX 77030, and Division of Cellular and Molecular Cardiology, Central Institute for Cardiovascular Research, Academy of Sciences of the GDR, Berlin-Buch, GDR.
A. M. J. VanDongen, G. E. Kirsch, A. M. Brown, Department of Molecular Physiology and Biophysics, Baylor College of Medicine, One Baylor Plaza, Houston, TX 77030.